Article

Improving of Thermoelectric Efficiency of Layered Sodium Cobaltite Through its Doping by Different Metal Oxides

Natalie S. Krasutskaya , Ekaterina A. Chizhova , Julia Yu. Zizika , Alexey V. Buka , Hongchao Wang , Andrei I. Klyndyuk *

Posted Date: 11 March 2025

doi: 10.20944/preprints202503.0767.v1

Keywords: thermoelectric oxides; layered sodium cobaltite; microstructure, electrical properties; thermal properties; figure-of-merit

Article

Improving of Thermoelectric Efficiency of Layered Sodium Cobaltite Through its Doping by Different Metal Oxides

Natalie S. Krasutskaya [1], Ekaterina A. Chizhova [1], Julia Yu. Zizika [2], Alexey V. Buka [3], Hongchao Wang [4] and Andrei I. Klyndyuk [1,5,*]

[1] Department of Physical, Colloid and Analytical Chemistry, Organic Substances Technology Faculty, Belarusian State Technological University, Sverdlova str. 13a, 220006 Minsk, Belarus

[2] Structural Analysis Sector, Physical-Technical Institute of the National Academy of Science of Belarus, Academician Kuprevich str. 10, 220084 Minsk, Belarus

[3] Department of Glass, Ceramics and Binding Materials Technology, Chemical Technology and Engineering Faculty, Belarusian State Technological University, Sverdlova str. 13a, 220006 Minsk, Belarus

[4] School of Physics, State Key Laboratory of Crystal Materials, Shandong University, Jinan, 250100, China

[5] Department of Physical Chemistry and Electrochemistry , Chemical Faculty, Belarusian State University, Nezavisimosti av. 4, 220030 Minsk, Belarus;

* Correspondence: klyndyuk@belstu.by; Tel.: +375 (29) 6365624

Abstract: Through the solid-state reactions method the $Na_{0.89}Co_{0.9}Me_{0.1}O_2$ (*Me* = Cr, Ni, Mo, W, Pb, Bi) ceramic samples were prepared and their crystal structure, microstructure, electrical, thermal and thermoelectric properties were investigated. The effect of nature of doping metal (*Me* = Cr, Ni, Mo, W, Bi) on the structure and properties of layered sodium cobaltite $Na_{0.89}CoO_2$ was analyzed. The largest Seebeck coefficient (616 (μV/K) at 1073 K) and figure-of-merit (1.74 at 1073 K) values among the samples studied demonstrated the $Na_{0.89}Co_{0.9}Bi_{0.1}O_2$ solid solution, which also characterized by lowest value of dimensionless relative self-compatibility factor about 8% within 673–873 K temperature range. The obtained results demonstrate that doping of layered sodium cobaltite by transition and heavy metal oxides improves its microstructure and thermoelectric properties, which showes the prospectiveness of used doping strategy for development of new thermoelectric oxides with improved thermoelectric characteristics.

Keywords: thermoelectric oxides; layered sodium cobaltite; microstructure; electrical properties; thermal properties; figure-of-merit

1. Introduction

About two-third of energy consumed by factories, transport, and households, is dissipated into environment and, in fact, lost for humanity [1]. This high-potential waste heat can be partially transferred into electrical energy using thermoelectrogenerators (TEGs). To produce TEGs one need so-called thermoelectric materials, which should possess a complex of unique properties, such as low electrical resistivity (ρ) and thermal conductivity (λ), high values of Seebeck coefficient (*S*) etc. [2–5]. Traditional thermoelectrics based on the layered chalcogenides of bismuth, lead etc. possess a number of drawbacks as they content toxic, rare and expensive components as well as unstable in air at elevated temperatures. These drawbacks are absent for oxide thermoelectrics [6–10], one of well-known representative of them is layered sodium cobaltite Na_xCoO_2, firstly described by Jansen and Hoppe [11] and characterized as thermoelectric by Terasaki et al. [12]. Its structure consists of $[CoO_2]$ layeres (CdI_2 structure) with sodium atoms in between them [13]. According to Viciu et al. [14], the concentration of oxygen vacancies in $[CoO_2]$ layers is negligible, so oxidation state of cobalt ions in it is only determined by the sodium content (x_{Na}). Due to its unique transport properties, Na_xCoO_2 is

 doi:10.20944/preprints202503.0767.v1

considered as potential material for *p*-branches of TEGs and ceramic (oxide) thermocouples [15,16], cathode material of sodium-ion batteries (SIBs) [17–20], and its crystal hydrate, $Na_xCoO_2 \cdot yH_2O$, below 4 K indergoes into a superconducting state [21]. Crystal structure, electrotransport, thermal, and functional characteristics of Na_xCoO_2 strongly depend on the sodium content in it [22–25].

Functional, including thermoelectric, characteristics of the ceramic samples of the layered sodium cobaltite are worse than for moncrystals, but they can be improved using different approaches: *i*) doping in sublattices of cobalt [26–28] or/and sodium [29–31], *ii*) modification by particles of metals [32,33] or semiconductors [34], *iii*) using so-called soft synthesis methods [7,35,36], *iiii*) using of special sintering techniques [37] resulting in improving of ceramics microstructure which enhances its electrotransport and mechanical properties.

Partial substitution of cobalt by copper in $NaCo_{2-x}Cu_xO_4$ ceramics improves its sinterability, lowers electrical resistivity and enhances Seebeck coefficient, resulting in essential increase of power factor values of these solid solutions comparing to the unsubstituted sodium cobaltite [38,39], which reache maximal value for $NaCo_{1.8}Cu_{0.2}O_4$ phase – 3.08 mW/(m·K²) at 1073 K [38]. Substitution of cobalt by nickel deteriorates sinterability of $NaCo_{2-x}Ni_xO_4$ phases, but decreases their ρ and strongly enlarges *S*, and *P* value for $NaCo_{1.9}Ni_{0.1}O_4$ at 1073 K reaches 2.36 mW/(m·K²), which is 8 times larger than for base $NaCo_2O_4$ phase [40,41]. When zinc substitutes cobalt in $NaCo_{2-x}Zn_xO_4$, electrical resistivity and Seebeck coefficient of ceramics increase, and power factor reaches 1.7 mW/(m·K²) at 1073 K for $NaCo_{1.9}Zn_{0.1}O_4$ solid solution, which is 4 times larger than for $NaCo_2O_4$ cobaltite [42].

Earlier we estimated the possibility to improve the thermoelectric performance of Na_xCoO_2 by increasing of sodium content in it [25] as well as by doping of sodium-poor $Na_{0.55}CoO_2$ cobaltite with oxides of different transition and non-transition metals [16,43].

In this work the effect of the nature of different transition or heavy metals partially substituting cobalt in the sodium-rich $Na_{0.89}CoO_2$ layered cobaltite on its crystal structure, microstructure, thermophysical, electrophysical, and thermoelectric (functional) properties was studied.

2. Materials and Methods

Ceramic samples of $Na_{0.89}Co_{0.90}Me_{0.10}O_2$ (*Me* = Cr, Ni, Mo, W, Pb, and Bi) materials were obtained using solid-state reaction method according to the reaction scheme:

$$1.335\ Na_2CO_3 + 0.3/x\ Me_xO_y + 0.9\ Co_3O_4 + (0.5325 - 0.15\ y/x)\ O_2 = \\ = 3\ Na_{0.89}Co_{0.90}Me_{0.10}O_2 + 1.335\ CO_2 \qquad (1)$$

The powders of Na_2CO_3 (99%), Co_3O_4 (99%), Cr_2O_3 (99%), NiO (99.99%), MoO_3 (99.99%), WO_3 (99.99%), PbO (99.99%), and Bi_2O_3 (99.99%) were taken in the ratio of Na : Co : *Me* = 1.2 : 0.9 : 0.1 (the excess of Na_2CO_3 in the initial mixture is taken to compensate for the loss of Na_2O from the samples during their thermal treatment and allows to obtain ceramics of the specified composition [25,44]). The powdered samples were milled in a planetary mill PM 100 Retsch (material of beakers and grinding balls – ZrO_2) for 90 minutes at 300 rpm with the addition of C_2H_5OH (~3–5 wt.%). The resulting slurries were air-dried at a temperature of 323 K, and then pressed into tablets with a diameter of 19 mm and a thickness of up to 5 mm. After that, the obtained samples were calcined in air for 12 hours at a temperature of 1133 K. Subsequently, after calcination, the blanks were ground in an agate mortar and re-milled in a planetary mill, then pressed into bars measuring 5 × 5 × 30 mm³ and tablets with a diameter of 15 mm and a thickness of 2–3 mm, which were sintered in air for 12 hours at a temperature of 1203 K [43].

The real sodium content (x_{Na}) and the average oxidation state of cobalt (Co^{+Z}) in the obtained ceramic materials were determined using iodometric [44] and reverse potentiometric titration [45], as well as spectrophotometrically according to the method described in [46] (see Supplementary Information).

The phase composition of the samples and calculation of the crystal lattice parameters of the $Na_{0.89}Co_{0.90}Me_{0.10}O_2$ layered cobaltites were performed by means of X-ray diffraction analysis (XRD) using Bruker D8 XRD Advance X-ray diffractometer (CuKα radiation (λ = 1.5406 Å)).

 doi:10.20944/preprints202503.0767.v1

The values of the coherent scattering area for the $Na_{0.89}Co_{0.90}Me_{0.10}O_2$ ceramics were calculated using the Debye–Scherrer equation (D_S) (2) [47] and the size-strain method (D_{SS}) (3) [48]

$$D_S = \frac{0.9 \cdot \lambda}{\beta \cdot \cos\Theta}, \quad (2)$$

$$(d \cdot \beta \cdot \cos\Theta) = \left(\frac{0.9 \cdot \lambda}{D_{SS}}\right) \cdot (d^2 \cdot \beta \cdot \cos\Theta) + \left(\frac{\varepsilon}{2}\right)^2, \quad (3)$$

where d is the interplanar distance, nm; β is the full width of the reflex at its half maxima, rad; Θ is the diffraction angle, °; ε is the microstrain.

The degree of crystallographic orientation of the grains of the $Na_{0.89}Co_{0.90}Me_{0.10}O_2$ ceramics was evaluated using the Lotgering factor according to Equation (4) [49]:

$$f = \frac{p - p_0}{1 - p_0}, \quad (4)$$

where $p = \Sigma I(00l)/\Sigma I(hkl)$ (ΣI is the sum of the counts of X-ray diffraction peaks of the synthesized samples); $p_0 = \Sigma I_0(00l)/\Sigma I_0(hkl)$ (ΣI_0 is the sum of the counts of X-ray diffraction peaks of the reference phase JCPDC #00-030-1182).

The apparent density of the $Na_{0.89}Co_{0.90}Me_{0.10}O_2$ ceramic samples (d_{EXP}) was determined based on their mass and geometric dimensions, and their total porosity (Π_t) was calculated as follows

$$\Pi_t = \left(1 - \frac{d_{EXP}}{d_{XRD}}\right) \cdot 100\%, \quad (5)$$

where d_{XRD} is the X-ray density of the samples, g/cm^3.

The open porosity of the sintered samples (Π_O) was determined by weighing the ceramic samples of $Na_{0.89}Co_{0.90}Me_{0.10}O_2$, which were saturated with ethyl acetate for 60 minutes under a vacuum of 25–30 Pa, and then weighed in ethyl acetate according to Equation (6):

$$\Pi_o = \frac{m_1 - m}{m_1 - m_2} \cdot 100\%, \quad (6)$$

where m is the mass of the dry ceramic sample, g; m_1 and m_2 are the masses of the sample saturated by the liquid ethylacetate at weighing in air and introduced into the liquid ethylacetate, respectively, g.

The microstructure and chemical composition of the $Na_{0.89}Co_{0.90}Me_{0.10}O_2$ samples were studied using scanning electron microscopy (SEM) by a Tescan MIRA 3 LMH scanning electron microscope equipped with an AZtecLIVE Advanced energy dispersive microanalysis system with a nitrogen-free Ultim Max 100 standard detector (Oxford Instruments Analytical Ltd., UK).

The thermal expansion, electrical resistivity (ρ) and Seebeck coefficient (S) of the sintered ceramics were measured in air within a temperature range of 323–1073 K using the methodology described in [39,50,51]. Values of the average linear thermal expansion coefficient (α, LTEC) were calculated from the linear parts of $\Delta l/l_0 = f(T)$ plots.

The thermal diffusivity (η) of the $Na_{0.89}Co_{0.90}Me_{0.10}O_2$ layered cobaltites was studied in a helium atmosphere over a temperature range of 323–1073 K using the LFA 457 Micro-Flash device (NETZSCH). The thermal conductivity (λ) of the $Na_{0.89}Co_{0.90}Me_{0.10}O_2$ sintered ceramics was calculated using the Equation (7).

$$\lambda = \eta \cdot d_{EXP} \cdot C_p, \quad (7)$$

where Cp – is heat capacity, calculated by the Dulong–Petit law, J/(g·K). Thus, according to the data of works [16,52], the heat capacity of layered sodium cobaltite near 300 K becomes slightly dependent on temperature and reaches a plateau.

 doi:10.20944/preprints202503.0767.v1

The phonon (λ_{ph}) and electron (λ_e) parts of the thermal conductivity of the $Na_{0.89}Co_{0.90}Me_{0.10}O_2$ ceramics were roughly approximated by Equations (8) and (9)

$$\lambda = \lambda_e + \lambda_{ph} \quad (8)$$

$$\lambda_e = \frac{L \cdot T}{\rho} \quad (9)$$

where L is Lorentz number (L=2.45·10^{-8} W·Ω·K^{-2}).

The values of the power factor (P) and figure of merit (ZT) of the $Na_{0.89}Co_{0.90}Me_{0.10}O_2$ solid solutions were calculated as follows

$$P = \frac{S^2}{\rho} \quad (10)$$

and

$$ZT = \frac{P \cdot T}{\lambda} \quad (11)$$

The self-compability factor (s) and the dimensionless relative self-compatibility factor (Δs) [53] for the $Na_{0.89}Co_{0.90}Me_{0.10}O_2$ ceramics were calculated using equations (12) and (13)

$$s = \frac{\sqrt{1+ZT}-1}{S \cdot T} \quad (12)$$

and

$$\Delta s = \frac{s_{max} - s_{min}}{s_{min}} \cdot 100\% . \quad (13)$$

3. Results and Discussion

The sodium content in the obtained samples (x_{Na}), determined by iodometry, reverse potentiometry, and spectrophotometry methods, was approximately 0.89 for all the investigated samples (Tables 1, S1). The average oxidation state of cobalt in the $Na_{0.89}Co_{0.90}Me_{0.10}O_2$ (*Me* = Cr, Co, Ni, Mo, W, and Bi) layered cobaltites varied within 2.78–3.23 (Tables 1, S1), increasing with the substitution of an acceptor character (Ni instead of Co) and decreasing with the substitution of a donor character (Mo, W, Pb, or Bi instead of Co), which was also observed for the $Na_{0.55}Co_{0.90}Me_{0.10}O_2$ samples in the study [16].

According to the XRD results, all the ceramic samples were single-phase, within the XRD accuracy. The ceramic samples of $Na_{0.89}Co_{0.90}Me_{0.10}O_2$ (*Me* = Cr, Ni, Mo, W, Bi) obtained in the study, like the base $Na_{0.89}CoO_2$ cobaltite, exhibited a hexagonal structure corresponding to the γ-Na_xCoO_2 phase structure [11,29,54–56] (Figure 1*a*).

The values of the lattice constants for the $Na_{0.89}Co_{0.90}Me_{0.10}O_2$ solid solutions varied within the ranges of a = 2.822–2.831 Å and c = 10.92–10.97 Å (Table 1), which are close to the parameters of the $Na_{0.89}CoO_2$ base cobaltite (a = 2.826 Å, c = 10.94 Å) [26,57,58]. As a result, the values of volume of the unit cell for the phases of $Na_{0.89}Co_{0.90}Me_{0.10}O_2$ with partial cobalt substitution by transition or heavy metals changed very little, but their axial ratio significantly decreased only with the substitution of cobalt by nickel in the $Na_{0.89}CoO_2$ structure. Thus, partial substitution of cobalt with other metals in the $Na_{0.89}CoO_2$ phase does not lead to significant changes in the size and shape of the unit cell for the $Na_{0.89}Co_{0.90}Me_{0.10}O_2$ (*Me* = Cr, Mo, W, and Bi) solid solutions compared to the unsubstituted phase of layered sodium cobaltite.

 doi:10.20944/preprints202503.0767.v1

Table 1. Values of sodium content (x_{Na}), the average oxidation state of cobalt (Co^{+Z}), lattice constants (a, c, c/a, V), Lotgering factor (f), size of the coherent scattering area obtained using the Debye–Scherrer equation (D_S) and the size-strain method (D_{SS}), microstrain (ε) and X-ray density (d_{XRD}) of $Na_{0.89}Co_{0.9}Me_{0.1}O_2$ (*Me* = Cr, Co, Ni, Mo, W, Pb, Bi) ceramic samples.

Me	x_{Na}	Co^{+Z}	*a*, Å	*c*, Å	*c*/*a*	*V*, Å³	*f*	*Ds*, *nm*	*Dss*, *nm*	ε×10⁴	d_{XRD}, g/cm³
Cr	0.893	3.11	2.825	10.93	3.870	75.53	0.90	69	62	3.43	4.86
Co	0.891	3.11	2.826	10.94	3.872	75.71	0.31	63	45	4.56	4.98
Ni	0.889	3.23	2.831	10.92	3.856	75.75	0.69	70	70	2.61	4.88
Mo	0.894	2.78	2.822	10.96	3.883	75.57	0.87	73	70	1.41	5.06
W	0.889	2.78	2.825	10.97	3.884	75.80	0.92	67	69	1.50	5.43
Pb	0.888	3.01	2.825	10.94	3.873	75.64	0.92	79	60	3.22	5.55
Bi	0.894	2.90	2.823	10.93	3.872	75.45	0.76	77	72	2.49	5.56

The apparent density values of the $Na_{0.89}Co_{0.90}Me_{0.10}O_2$ ceramic ranged within 3.18–3.47 g/cm³ and decreased with the partial substitution of Co with Cr, Mo, W, or Pb, while they increased with the substitution of Co with Ni and Bi (Table 2). The values of open porosity of the ceramics varied within 16%–22% and were close for samples with different cationic compositions, but values of closed porosity were minimal for the base $Na_{0.89}CoO_2$ phase (13%) and $Na_{0.89}Co_{0.90}Ni_{0.10}O_2$ solid solution (7%) and for other samples varied within 17–24% and were close each other (Table 2).

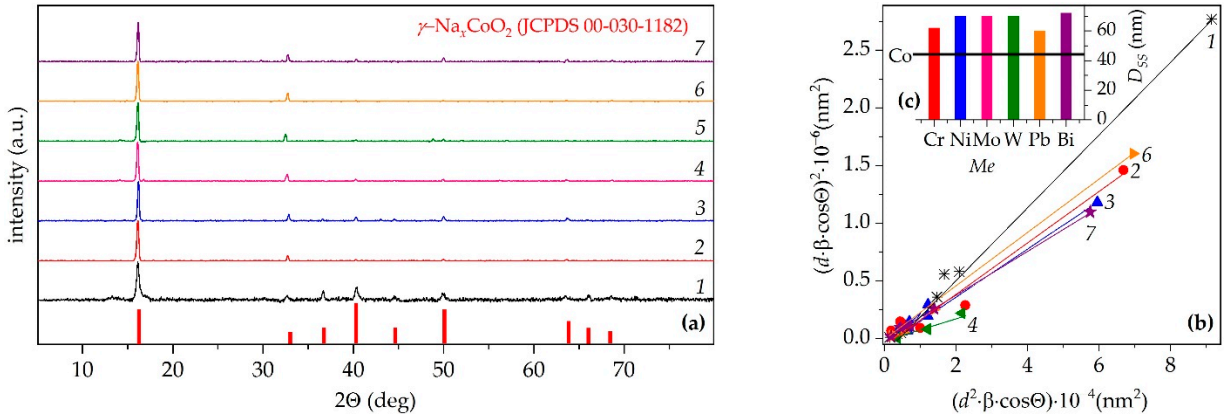

Figure 1. X-ray powder diffractograms ($Cu_{K\alpha}$–radiation) (a), size-strain plots (b) and coherent scatting area (c) for $Na_{0.89}CoO_2$ (*1*) layered sodium cobaltite and $Na_{0.89}Co_{0.9}Me_{0.1}O_2$ (*Me* = Cr (*2*), Ni (*3*), Mo (*4*), W (*5*), Pb(*6*), Bi (*7*)) solid solutions.

The values of the Lotgering factor increased from 0.31 for the $Na_{0.89}CoO_2$ base cobaltite (moderate orientation) to 0.69–0.76 for the $Na_{0.89}Co_{0.90}Me_{0.10}O_2$ solid solutions (*Me* = Ni and Bi) (good orientation) and 0.87–0.92 for the $Na_{0.89}Co_{0.90}Me_{0.10}O_2$ (*Me* = Cr, Mo, W, and Pb) ceramics of composition (very good orientation) (Table 1). Thus, doping $Na_{0.89}CoO_2$ with various transition or heavy metal oxides increases the degree of crystallographic orientation of the ceramic grains (the degree of its texturing). The most pronounced effect among the samples synthesized in this work was observed for $Na_{0.89}Co_{0.90}W_{0.10}O_2$, with the partial substitution of cobalt by tungsten in the $Na_{0.55}CoO_2$ phase leading to a similar effect [16,43].

The coherent scattering area of the $Na_{0.89}Co_{0.90}Me_{0.10}O_2$ materials, synthesized in the study, calculated using different approaches (Figure 1*b*), was larger (up to 6–25% and 3360% according to the Debye–Scherrer and the size-strain method, respectively) comparing to the base layered sodium cobaltite phase (Figure 1*b*, Table 1). In turn, the values of microstrains for the $Na_{0.89}Co_{0.90}Me_{0.10}O_2$ ceramics were slightly (*Me* = Cr and Pb) or significantly (*Me* = Ni, Mo, W, and Bi) lower compared to the initial $Na_{0.89}CoO_2$ cobaltite (Table 1). So, partial substitution of cobalt by transition or heavy metals

 doi:10.20944/preprints202503.0767.v1

in $Na_{0.89}CoO_2$ results in formation of ceramics possess the grains with larger dimensions and less strained.

According to the results of SEM, the grains of the $Na_{0.89}CoO_2$ base unsubstituted cobaltite had a plate-like shape with dimensions (*l*) of 6 – 15 μm and a thickness of 2.5 – 3 μm (with an average size (l_{av}) of about 7 μm and an aspect ratio (*AR*) of approximately 3.9) (Figure 2*b*). The microstructure of the $Na_{0.89}Co_{0.90}M_{0.10}O_2$ materials was similar to that of $Na_{0.89}CoO_2$, but it differed in the size and aspect ratio (shape) of the grains (Figures 2*a*, *c*–*f*).

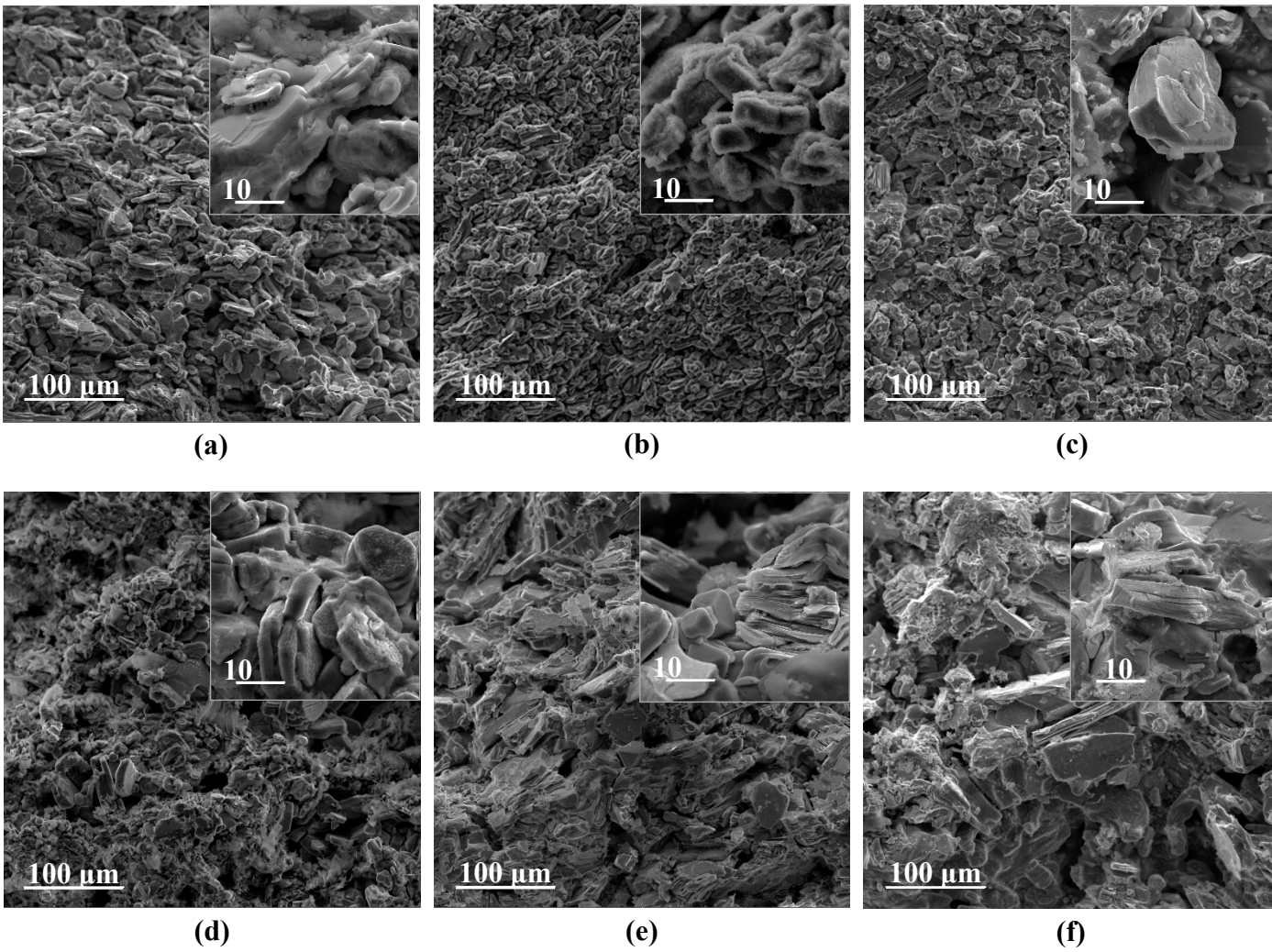

Figure 2. Electronic micrographs of ceramic cleavage of $Na_{0.89}Co_{0.9}M_{0.1}O_2$ (M = Cr (a), Co (b), Ni (c), W (d), Pb (e), Bi (f)).

The grain sizes of the $Na_{0.89}Co_{0.90}Me_{0.10}O_2$ (*Me* = Cr, Ni, W) ceramics varied within 6–23 μm with a thickness of 6–10 μm. The average dimension (l_{av} (*AR*)) was approximately 17 μm (2.8) for *Me* = Cr, 22 μm (3.3) for *Me* = Ni and 14 μm (3.2) for *Me* = W. Doping of the layered sodium cobaltite ceramics with bismuth or lead oxides resulted in an increase in grain size to 35–60 μm and decrease of the thickness of the grains by up to 1–3 μm. For $Na_{0.89}Co_{0.90}Pb_{0.10}O_2$ and $Na_{0.89}Co_{0.90}Bi_{0.10}O_2$, the l_{av} (*AR*) values were around 43 μm (14.3) and 52 μm (15.6), respectively. Consequently, the anisotropy of the grains in the sodium cobaltite ceramic increased with doping by heavy metal oxides (PbO_2, Bi_2O_3).

Enhancing of Lotgering factor and improving of anisotropy degree (*AR*) of the grains of $Na_{0.89}Co_{0.90}Me_{0.10}O_2$ ceramics may causes both by the differences in the sizes of subsituting and substituted ions (size effect) and in their charges (charge redistribution). The first results in localized lattice strain promoting preferential alignment of grains along specific crystallographic planes (in our

 doi:10.20944/preprints202503.0767.v1

case, (00*l*)), but the second alters charge distribution in the structure of $Na_{0.89}Co_{0.90}Me_{0.10}O_2$ phases, enhances interlayer charge screening, reduces electrostatic repulsion of CoO_2-layers, and stabilizes (00*l*)-oriented stacking. The maximal values of *f* and *AR* were observed, in the whole, for the samples of layered sodium cobaltite, doped by heavy metal oxides (Pb, W etc.) (Table 1, Figure 2), as namely in these cases maximal difference in the sizes and charges of substituting and substituted ions take place.

According to EDX results, the cationic composition of the $Na_{0.89}Co_{0.90}M_{0.10}O_2$ synthesized compounds was close to the target values, and the distribution of elements within the ceramic was nearly uniform (Figure 3, Figure *S*2 (see Supplementary Information)).

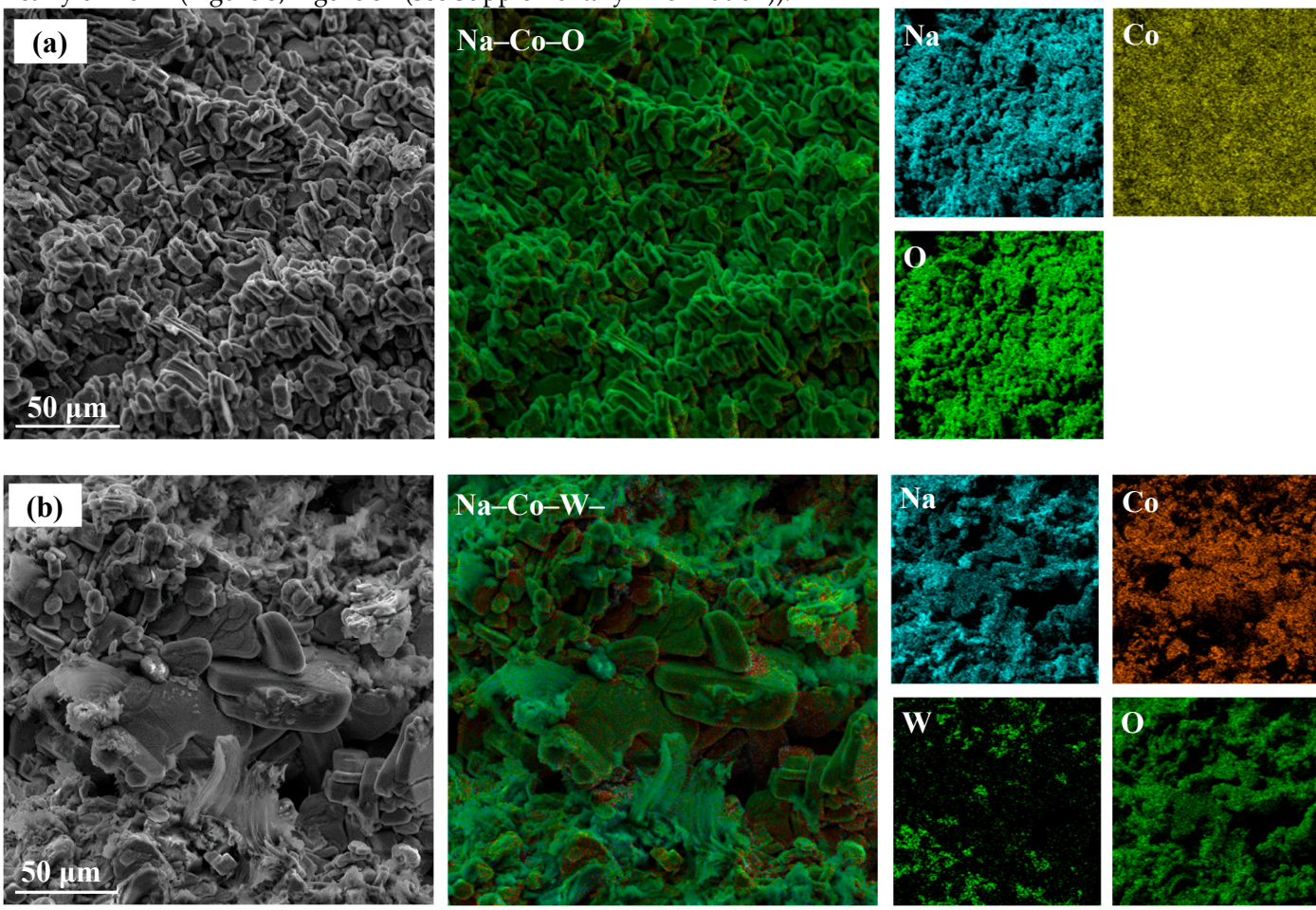

Figure 3. Element mapping images of the $Na_{0.89}CoO_2$ (a) and $Na_{0.89}Co_{0.9}W_{0.1}O_2$ (b) ceramic samples.

Temperature dependences of the relative elongation of $Na_{0.89}Co_{0.9}Me_{0.1}O_2$ ceramic samples were linear practically, which proves the absence of the structural phase transitions in the complex oxides investigated within all the temperature interval studied. LTEC values of the $Na_{0.89}Co_{0.9}Me_{0.1}O_2$ solid solutions varied within $(1.25–1.68)\cdot10^{-5}$ K^{-1} and were lower (for *Me* = Pb, and Bi), slightly (for Me = W) and essentially larger (for Me = Cr, Ni, and Mo) than for unsubstituted sodium cobaltite $Na_{0.89}CoO_2$ ($1.34\cdot10^{-5}$ K^{-5}) (Table 2).

Obtained increasing of LTEC values of $Na_{0.89}Co_{0.90}Me_{0.10}O_2$ derivatives in comparison to the $Na_{0.89}CoO_2$ base phase possibly is due to the high values of their porosity (Table 2) as well as to the increasing of anharmonicity degree of metal–oxygen vibrations in their structure at partial substitution of cobalt by other metals.

 doi:10.20944/preprints202503.0767.v1

Table 2. Values of apparent (d_{EXP}) density, total ($П_t$), open ($П_o$) and closed ($П_c$) porosity, linear thermal expansion coefficient (α), electrical resistivity ($ϱ_{1073}$), Seebeck coefficient (S_{1073}), power factor (P_{1073}) and figure-of-merit (ZT_{1073}) of $Na_{0.89}Co_{0.9}Me_{0.1}O_2$ (*Me* = Cr, Co, Ni, Mo, W, Pb, Bi) ceramics.

M	d_{EXP}, g/cm³	$П_t$, %	$П_o$, %	$П_c$, %	$10^5 \times \alpha$, K⁻¹	$10^4 \times ϱ_{1073}$, Ω·m	S_{1073}, μV/K	P_{1073}, mW/(m·K²)	λ_{1073}, W/(m·K)	ZT_{1073}
Cr	3.18	35	16	19	1.68	3.28	134	0.055	0.613	0.10
Co	3.38	32	19	13	1.34	2.43	439	0.794	0.536	1.59
Ni	3.46	29	22	7	1.42	1.50	369	0.910	0.591	1.65
Mo	3.22	36	19	17	1.47	5.73	408	0.291	0.323	0.97
W	3.20	41	17	24	1.39	10.9	519	0.320	0.316	1.09
Pb	3.34	40	18	22	1.26	5.58	358	0.230	0.295	0.84
Bi	3.47	38	18	20	1.25	5.97	616	0.636	0.392	1.74

As can be seen from the Figure 4*a*, the $Na_{0.89}CoO_2$ layered sodium cobaltite and its $Na_{0.89}Co_{0.90}Me_{0.10}O_2$ derivatives exhibited metallic-like conductivity character ($\partial ϱ/\partial T>0$) (except $Na_{0.89}Co_{0.90}W_{0.10}O_2$ solid solution, which possesses semiconducting conductivity character within all the temperature interval studied), which for the $Na_{0.89}Co_{0.90}Bi_{0.10}O_2$ and $Na_{0.89}Co_{0.90}Mo_{0.10}O_2$ solid solutions near 923 K changed into a semiconducting one ($\partial ϱ/\partial T<0$) like the conductivity crossover in layered calcium cobaltite of $Ca_3Co_4O_{9+\delta}$ [60,61]. A similar effect was also observed in several $Na_{0.55}Co_{0.90}Me_{0.10}O_2$ layered sodium cobaltites earlier [16]. The doping of $Na_{0.89}CoO_2$ layered sodium cobaltite by different metal oxides results in increasing its electrical resistivity values, except NiO, as ρ values of $Na_{0.89}Co_{0.90}Ni_{0.10}O_2$ solid solution were essentially less than for the unsubstituted layered sodium cobaltite (Figure 4*a*, *d*). As can be seen, electrical resistivity values of ceramics increased at increasing of oxidation state of the substituting cobalt metal *Me* ($ϱ(Na_{0.89}Co_{0.90}Ni_{0.10}O_2) < ϱ(Na_{0.89}CoO_2) < ϱ(Na_{0.89}Co_{0.90}Pb_{0.10}O_2)$). This can be explained by a decrease in the concentration of main charge carriers (holes) as the average oxidation state of cations in the conducting $(Co,Me)O_2$ layers of the crystal structure $Na_{0.89}Co_{0.90}Me_{0.10}O_2$ phases increases (Figure 4*a*, *d*, Table 2).

The Seebeck coefficient of the $Na_{0.89}Co_{0.90}Me_{0.10}O_2$ (*Me* = Cr, Ni, Mo, W, Pb, and Bi) solid solutions was positive throughout the temperature range studied, indicating that the main charge carriers are holes, and these materials are classified as *p*-type conductors. It is also noteworthy that at high temperatures, the change in thermo-EMF for all materials studied was nearly linear. This relationship of the Seebeck coefficient corresponds to Equation (14), which is commonly used to describe the thermoelectric properties of metals and degenerate semiconductors [62]

$$S = \left(\frac{8 \cdot \pi^2 \cdot k_B^2}{3 \cdot e \cdot h}\right) \cdot m^* \cdot T \cdot \left(\frac{\pi}{3 \cdot n}\right)^{2/3}, \quad (14)$$

where k_B is the Boltzmann constant, J/K; m^* is the density of a state effective mass, kg; *h* is the Planks constant, J·s; *e* is the charge of the electron, C; *T* is the absolute temperature, K; *n* is the charge carrier's concentration, cm^{-3}.

Partial substitution of cobalt with ions of various transition or heavy metals in the structure of $Na_{0.89}CoO_2$ leads to an increase in its Seebeck coefficient, which is more pronounced at high temperatures for tungsten- or bismuth-substituted solid solutions (Figure 4*b*,*e* and Table 2). This is likely due to the increase in configurational entropy provided by the presence of cobalt ions in different charge (Co^{2+}, Co^{3+}, and Co^{4+}) and spin states (high-, intermediate-, and low-spin). The highest values of S among all investigated samples were demonstrated by the $Na_{0.89}Co_{0.90}W_{0.10}O_2$ and $Na_{0.89}Co_{0.90}Bi_{0.10}O_2$ oxides (519 and 616 μV/K at 1073 K, respectively), which are 1.18 and 1.40 times larger than that of the parent $Na_{0.89}CoO_2$ phase (Figure 4*e* and Table 2). So, these phases can be considered as prospective materials for *p*-legs of ceramic (oxide) thermocouples. It should also be

 doi:10.20944/preprints202503.0767.v1

noted that similar results were obtained when studying the Seebeck coefficient of cobalt-substituted derivatives of the $Na_{0.55}CoO_2$ layered cobaltite [16,38].

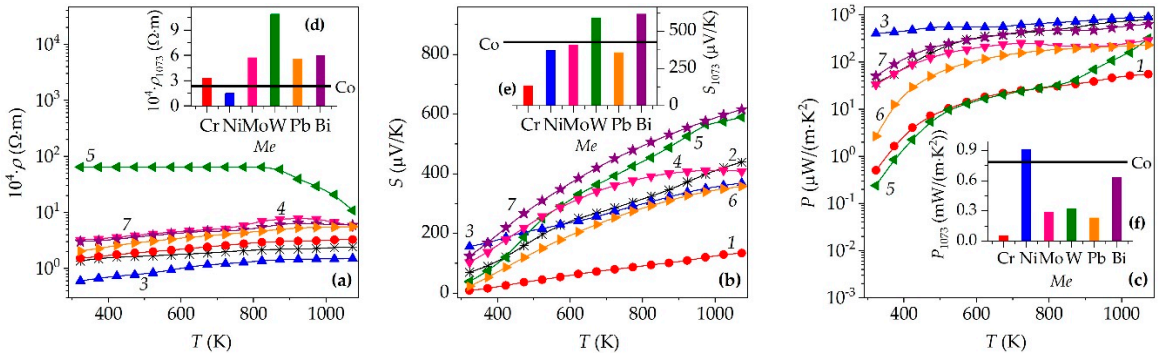

Figure 4. Temperature dependences of electrical resistivity ρ (a), Seebeck's coefficient S (b) and power factor P (c) of ceramic samples of $Na_{0.89}Co_{0.9}Me_{0.1}O_2$ (Me = Cr (1), Co (2), Ni (3), Mo (4), W (5), Pb (6), Bi (7)). Insets show the electrical resistivity ρ_{1073} (d), Seebeck's coefficient S_{1073} (e) and power factor P_{1073} (f) values of $Na_{0.89}Co_{0.9}Me_{0.1}O_2$ phases.

Value of weighted mobility (μ_p) and concentration (p) of the main charge carriers («holes») in the samples studied, calculated on the base of experimentally determined ρ and S values according to the methodics described in [63] (see Supplementary Information, Equations (S8) and (S9)), varied with temperature changing and essentially and nonmonotonously changed when $Na_{0.89}CoO_2$ was doped by different metal oxides. For the base $Na_{0.89}CoO_2$ cobaltite at 1073 K values of μ_p and p were equal ~48 $cm^2/(V \cdot s)$ and ~$5 \cdot 10^{-20}$ cm^{-3} respectively which is in a good accordance with the literature date [63]. Weighted mobility values of the $Na_{0.89}Co_{0.90}Me_{0.10}O_2$ solid solutions were less, close to, end large, than for $Na_{0.89}CoO_2$ for Me = Cr, Mo, Pb, Me = Ni, W, and Me = Bi respectively. Charge carriers concentration in $Na_{0.89}Co_{0.90}Me_{0.10}O_2$ cobaltites was large, close to, and less, than for $Na_{0.89}CoO_2$ phase for Me = Cr, Me = Mo, Ni, Pb, and Me = W, Bi respectively, that is in good accordance with the results of measurements of Seebeck coeffisient of ceramics, for example, with the sharp increasing of S values of the layred sodium cobaltite at partical substitution of cobalt by bismuth or tungsten in it, and with the scharp decreasing of S at partical substitution of cobalt by chromium in $Na_{0.89}CoO_2$ (Figure 4*b*,*e*).

The power factor values of $Na_{0.89}Co_{0.90}Me_{0.10}O_2$ sintered ceramics increased with rising temperature and changed non-monotonically with the changing of nature of metal substituting cobalt in the $Na_{0.89}CoO_2$ structure (Figure 4*c*,*f* and Table 2). The maximum P value was achieved for the $Na_{0.89}Co_{0.90}Ni_{0.10}O_2$ nickel-substituted solid solution (0.910 $mW/(m \cdot K^2)$ at 1073 K), which is 1.15 times larger than that of the undoped $Na_{0.89}CoO_2$ layered sodium cobaltite, and was determined both by low values of its electrical resistivity and high values of its Seebeck's coefficient.

The thermal diffusivity and thermal conductivity values of the $Na_{0.89}Co_{0.10}Me_{0.10}O_2$ ceramics decreased with increasing of temperature (Figure 5*a*,*b*) and changed nonmonotonously at the doping of $Na_{0.89}CoO_2$ by various metal oxides, increasing at substitution of Co by Cr, and Ni, and decreasing at substitution of Co by Mo, W, Pb, and Bi (Figure 5*d*,*e*). The first is perhaps associated with an increase in the grain size of the ceramics, which led to a decrease in the density of grain boundaries that serve as effective phonon scattering regions, but the last took place due to the partial replacing of lighter cobalt ion by heavier ions of molibdenium, tungsten, lead, or bismuth, serving as effective scattering centers. The electronic part of the thermal conductivity of the ceramics was relatively small (λ_e/λ=0.03–0.13) and increased with the rising of temperature, and for the $Na_{0.89}Co_{0.10}Me_{0.10}O_2$ solid solutions, except $Na_{0.89}Co_{0.90}Ni_{0.10}O_2$ one, it was lower than that of the $Na_{0.89}CoO_2$ base oxide. Thus, the main part of the heat in the $Na_{0.89}Co_{0.10}Me_{0.10}O_2$ phases was carried by lattice vibrations (phonons) ($\lambda_{ph}/\lambda \approx$(0.87–0.97)) (Figure 5*c*,*f*). As can be seen from the Figure 5, both thermal diffusivity and conductivity values of the doped cobaltites (except Cr- and Ni-doped) are less than that of the base $Na_{0.89}CoO_2$ phase. It should be noted, that for sodium-poor samples ($Na_{0.55}Co_{0.90}Me_{0.10}O_2$) the

 doi:10.20944/preprints202503.0767.v1

contraversal effect was found, namely increasing of η and λ values of doped with transition or heavy metal oxides ceramics comparing to the undoped $Na_{0.55}CoO_2$ phase [16,38].

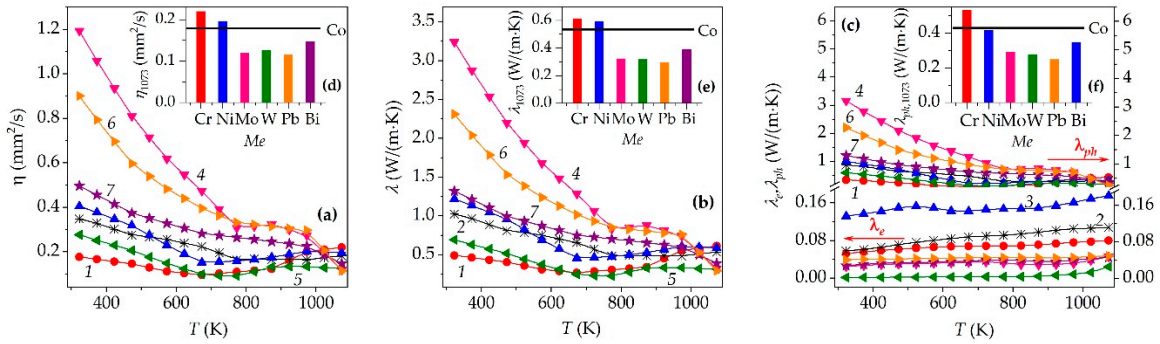

Figure 5. Temperature dependences of thermal diffusivity η (*a*), total thermal conductivity λ (b), phonon λ_{ph} and electron λ_e contributions (c) in thermal conductivity of $Na_{0.89}Co_{0.9}Me_{0.1}O_2$ (*Me* = Cr (1), Co (2), Ni (3), Mo (4), W (5), Pb (5), Bi (6)) ceramic samples. Insets show the thermal diffusivity η_{1073} (d), total thermal conductivity λ_{1073} (e) and phonon thermal conductivity $\lambda_{ph,1073}$ of $Na_{0.89}Co_{0.9}M_{0.1}O_2$ materials.

Figure of merit values of the investigated materials sharply increased with rising temperature, and doping of layered sodium cobaltite with various transition and heavy metal oxides had different effect – ZT increased at substitution in $Na_{0.89}CoO_2$ of cobalt by nickel and bismuth and decreased when cobalt was partially substituted by chromium, molibdenium, tungsten, and lead (Figure 6*a* and Table 2). The highest thermoelectric characteristics were demonstrated by $Na_{0.89}Co_{0.90}Ni_{0.10}O_2$ and $Na_{0.89}Co_{0.90}Bi_{0.10}O_2$ solid solutions, with *ZT* values reaching 1.65 and 1.74 at 1073 K, which is about 4% and 9% respectively higher than that of the $Na_{0.89}CoO_2$ phase (Figure 6*c*). It should be noted, that though for the $Na_{0.89}Co_{0.90}W_{0.10}O_2$, $Na_{0.89}Co_{0.90}Mo_{0.10}O_2$ and $Na_{0.89}Co_{0.90}Pb_{0.10}O_2$ ceramics *ZT* values were less than for $Na_{0.89}CoO_2$ phase, at 1073 K they were equal to 1.09, 0.97, and 0.84 respectively, which is close to the theoretical criterion ($ZT > 1$) that defines materials of practical interest for thermoelectric conversion (Figure 6*a* and Table 2).

The self-compatibility factor values (*s*) of the ceramics studied increased at temperature increasing and within temperature interval 673–873 K slightly vary (except for $Na_{0.89}Co_{0.90}Cr_{0.10}O_2$ compound) (Figure 6*b*), and dimensionless relative self-compatibility factor (Δs) of $Na_{0.89}Co_{0.90}Me_{0.10}O_2$ layered cobaltites within 673–873 K varies within 8–29% (Figure 6*d*), which is, in the whole, less than for the $Mg_2Si_{0.6-y}Sn_{0.4}Sb_y$ (25-40%) thermoelectric alloy [64] and states the good self-compatibility of the obtained in this work thermoelectric oxide ceramics. Note, that Δs values for the doped sodium cobaltites, except $Na_{0.89}Co_{0.90}Mo_{0.10}O_2$, were less (8–21%) than for the base layered sodium cobaltite (26%), which shows the effectiveness of doping of $Na_{0.89}CoO_2$ by transition or heavy metal oxides in increasing of its self-compatibility.

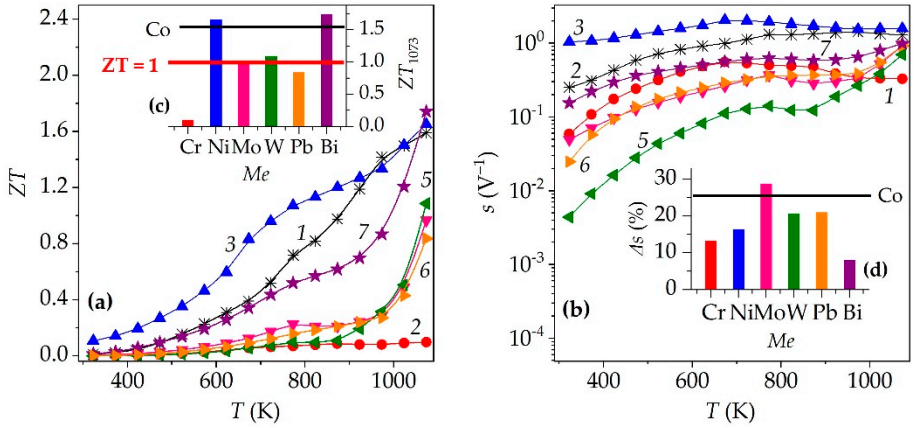

 doi:10.20944/preprints202503.0767.v1

Figure 6. Temperature dependences of figure-of-merit *ZT* (a) and self-compability factor *s* (b) of $Na_{0.89}Co_{0.9}Me_{0.1}O_2$ (*Me* = Cr (1), Co (2), Ni (3), Mo (4), W (5), Pb (6), Bi (7)) ceramic samples. Insets show the figure-of-merit ZT_{1073} (c) and dimensionless relative self-compatibility factor $\Delta s_{673–873K}$ (d) (within 673–873 K temperature range) of $Na_{0.89}Co_{0.90}Me_{0.10}O_2$ ceramics.

4. Conclusions

Combining the obtained in this study results one can conclude that doping (up to 10 mol.%) of $Na_{0.89}CoO_2$ layered soldium cobaltite by different transition (Cr_2O_3, NiO) and heavy metal oxides (MoO_3, WO_3, PbO, Bi_2O_3) did not changed its crystal structure and slightly affects its lattice constants values, but increasing coherent scattering area, grain size as well as grain orientation degree of $Na_{0.89}Co_{0.10}Me_{0.10}O_2$ solid solutions comparing to the parent $Na_{0.89}CoO_2$ phase.

Such a doping lead, in the whole, to the decrease of elecrical resistivity of the samples and complex changing of Seebeck cofficient and thermal properties of the ceramics, which determined both the nature of metal substituting cobalt in the $Na_{0.89}CoO_2$ and the peculiarities of the microstructure of the ceramics. The maximal values of S possess the $Na_{0.89}Co_{0.90}W_{0.10}O_2$ and $Na_{0.89}Co_{0.90}Bi_{0.10}O_2$ cobaltites (519 and 616 μV/K at 1073 K, respectively), which are 18% and 40% higher than that of the parent $Na_{0.89}CoO_2$ phase. So, these materials can be recommended as potential materials for *p*-legs of ceramic thermocouples.

Maximal power factor was observed for the $Na_{0.89}Co_{0.90}Ni_{0.10}O_2$ compound (0.910 mW/(m·K²) at 1073 K), which is 15% higher than that of the base $Na_{0.89}CoO_2$ layered sodium cobaltite, and was determined both by low values of its electrical resistivity and high values of its Seebeck's coefficient. The maximal thermoelectric performance demonstrate the $Na_{0.89}Co_{0.90}Ni_{0.10}O_2$ and $Na_{0.89}Co_{0.90}Bi_{0.10}O_2$ phases, which *ZT* values is equal 1.65 and 1.74 at 1073 K, that is about 4% and 9% respectively higher than for $Na_{0.89}CoO_2$ phase. So, these materials can be considered as potential materials for the *p*-branches of the modules of high-temperature thermoelectrogenerators.

The obtained results demonstrate the effectiveness of the doping strategy of cobalt by heavy metals in layered sodium cobaltite for the enhancement of the thermoelectric performance of its derivatives. It was also found that dimensionless relative self-compatibility factor of the $Na_{0.89}CoO_2$ layered sodium cobaltite essentially reduced at its doping by transition or heavy metal oxides.

Supplementary Materials: The following supporting information can be downloaded at the website of this paper posted on Preprints.org, Figure S1: Absorption spectra and calibration graphs for determining cobalt content in the form of complexes $[Co(SCN)_4]^{2-}$(*a*, *c*) и $[CoY]^-$ (*b*, *d*); Figure S2: Element mapping images of the $Na_{0.89}Co_{0.90}M_{0.10}O_2$ ceramic samples (M = Cr (*a*), Ni (*b*), Pb (*c*), Bi (*d*)); Table S1: Sodium content (x_{Na}) and average oxidation state of cobalt (*Z*) in $Na_{0.89}Co_{0.90}M_{0.10}O_2$ layered cobaltites samples determined by various methods.

Author Contributions: Conceptualization, A.I.K.; methodology, A.I.K., E.A.C. and N.S.K.; software, N.S.K.; validation, A.I.K., E.A.C., H.W.; formal analysis, N.S.K., E.A.C.; investigation, N.S.K., Y.A.Z., A.V.B.; resources, A.I.K.; data curation, A.I.K.; writing—original draft preparation, N.S.K., A.I.K.; writing—review and editing, A.I.K., H.W.; visualization, N.S.K.; supervision, A.I.K.; project administration, A.I.K.; funding acquisition, A.I.K., N.S.K. All authors have read and agreed to the published version of the manuscript.

Funding: This work was supported by the Ministry of Education of the Republic of Belarus, under project number 20111575, and by the Belarusian Republican Foundation for Fundamental Research, under project number 20122443.

Data Availability Statement: All data generated or analyzed during this study are included in this published article.

Acknowledgments: The authors would like to thank Dzmitry S. Kharytonau for fruitful discussions of research results and Dzmitry Darashchuk for technical support.

Conflicts of Interest: The authors declare no conflict of interest.

References

1. Klyndyuk, A.I.; Kharytonau, Dz.S.; Matsukevich, I.V.; Chizhova, E.A.; Lenčéš, Z.; Socha, R.P.; Zimowska, M.; Hanzel, O.; Janek, M. Effect of cationic nonstoichiometry on thermoelectric properties of layered

 doi:10.20944/preprints202503.0767.v1

calcium cobaltite obtained by field assisted sintering technology (FAST). *Ceramics International*. **2024**, *50*, 30970–30979. https://doi.org/10.2139/ssrn.4777166

2. Polevik, A.O.; Sobolev A.V.; Glazcova, Ia.S.; Presniakov, I.A.; Verchenko, V.Yu.; Link, J.; Stern, R.; Shevelkov, A.V. Interplay between Fe(II) and Fe(III) and Its Impact on Thermoelectric Properties of Iron-Substituted Colusites $Cu_{26-x}Fe_xV_2Sn_6S_{32}$. *Compounds*. **2023**, *3*, 348–364. https://doi.org/10/3390/compounds3020027.
3. Yu, J.; Chen, K.; Azough, F.; Alvarez-Ruiz, D.T.; Reece, M.I.; Freer, R. Enhancing the thermoelectric performance of calcium cobaltite ceramics by tuning composition and processing. *ACS Applied Materials Interfaces*. **2020**, *12*, 47634–47646. https://doi.org/10.1021/acsami.0c14916.
4. Zhang, W.; Zhu, K.; Liu, J.; Wang, J.; Yan, K.; Liu, P.; Wang, Y. Influence of the phase transformation in Na_xCoO_2 ceramics on thermoelectric properties. *Ceramics International*. **2018**, *44*, 17251–17257. https://doi.org/10.1016/j.ceramint.2018.06.183.
5. Li, Z.; Xiao, C.; Xie, Y. Layered thermoelectric materials: Structure, bonding, and performance mechanisms. *Applied Physics Review*. **2020**, *9*, 011303. https://doi.org/10.1063/5.0074489.
6. Kuzanyan, A.S.; Margani, N.G.; Zhghamadze, V.V.; Mumladze, G.; Badalyan, G.R. Impact of $Sr(BO_2)_2$ Dopant on Power Factor of $Bi_2Sr_2Co_{1.8}O_y$ Thermoelectric. *Journal of Contemporary Physics*. **2021**, 56, 146–149.
7. Oopathumpa, Ch.; Boonthuma, D.; Smith, S. M. Effect of Poly(Vinyl Alcohol) on Thermoelectric Properties of Sodium Cobalt Oxide. *Key Engineering Materials*. **2019**, *798*, 304–309. https://doi.org/10.4028/www.scientific.net/KEM.798.304.
8. Mallick, M.M.; Vitta, V. Enhancing Thermoelectric Figure-of-Merit of Polycrystalline Na_yCoO_2 by a Combination of Non-stoichiometry and Co-substitution. *Journal of Electronic Materials*. **2018**, *47*, 3230–3237. https://doi.org/10.1007/s11664-018-6186-9.
9. Yu,J.; Chang, Y.; Jakubczyk, E.; Wang, B.; Azough, F.; Dorey, R.; Freer, R.; Modulation of electrical transport in calcium cobaltite ceramics and thick films through microstructure control and doping. *Journal of the European Ceramic Society*. **2021**, *41*, 4859–4869. https://doi.org/10.1016/j.jeurceramsoc.2021.03.044.
10. Noudem, J.G.; Xing, Yi. Overview of Spark Plasma Texturing of Functional Ceramics. *Ceramics*. **2021**, *4*, 97–107. https://doi.org/10.3390/ceramics4010009.
11. Jansen, M.; Hoppe, R. Notiz zur Kenntnis der Oxocobaltate des Natriums. *Zeitschrift für anorganische und allgemeine Chemie*. **1974**, *408*. 104–106. https://doi.org/10.1002/zaac.19744080203.
12. Terasaki, I.; Sasago, Y.; Uchinokura, K. Large thermoelectric power in $NaCo_2O_4$ single crystals. *Physical Review B*. **1997**, *56*. R12685–R12687. https://doi.org/10.1103/PhysRevB.56.R12685.
13. Koumoto, K.; Terasaki, I.; Funahashi, R. Complex Oxide Materials for Potential Thermoelectric Applications. *MRS BULLETIN*. **2006**, *31*, 206–210. https://doi.org/10.1557/mrs2006.46.
14. Viciu L., Huang Q., Cava R.J. Stoichiometric oxygen content in Na_xCoO_2 // *Physical Review B*. **2006**, *73*. 212107 (4 pages). https://doi.org/10.1103/PhysRevB.73.212107.
15. Han, Yu.; Ruan, Yo.; Xue, M.; Shi, M.; Song, Zh.; Zhou, Yua.; Teng, J. Effect of Annealing Time on the Cyclic Characteristics of Ceramic Oxide Thin Film Thermocouples. *Micromachines*. **2022**, *13*, 1970 (9 pages). https://doi.org/10.3390/mi13111970.
16. Krasutskaya, N.S.; Klyndyuk, A.I.; Evseeva, L.E.; Gundilovich, N.N.; Chizova, E.A.; Paspelau, A.V. Enhanced thermoelectric performance of $Na_{0.55}CoO_2$ ceramics doped by transition and heavy metal oxides. *Solids*. **2024**, *5*, 267–277. https://doi.org/10.3390/solids5020017.
17. Molenda, J.; Baster, D.; Milewska, A.; Świerczek, K.; Bora, D.K.; Braun, A.; Tobola, J. Electronic origin of difference in discharge curve between Li_xCoO_2 and Na_xCoO_2 cathodes. *Solid State Ionics*. **2014**, *271*, 15–27. https://doi.org/10.1016/j.ssi.2014.09.032.
18. Pohle, B.; Gorbunov, M.; Lu, Q.; Bahrami, A.; Nielsch, K.; Mikhailova, D. Structural and electrochemical properties of layered *P*2-$Na_{0.8}Co_{0.8}Ti_{0.2}O_2$ cathode in sodium-ion batteries. *Energies*. **2022**, *15*, 3371. https://doi.org/10.3390/en15093371.
19. Nguyen, L.M.; Nguyen, V.H.; Nguyen, D.M.N.; Le, M.K.; Tran, V.M.; Le, M.L.P. Evaluating electrochemical properties of layered $Na_xMn_{0.5}Co_{0.5}O_2$ obtained at different calcined temperatures. *Chemengineering*. **2023**, *7*, 33. https://doi.org/10.3390/chemengineering7020033.

20. Baster, D.; Zając, W.; Kondracki, Ł.; Hartman, F.; Molenda, J. Improvement of electrochemical performance of $Na_{0.7}Co_{1-y}Mn_yO_2$–cathode material for rechargeable sodium-ion batteries. *Solid State Ionics*. **2016**, *288*, 213–218. https://doi.org/10.1016/j.ssi.2016.01.003.18.
21. Banobre-López, M.; Rivadulla, F.; Caudillo, R.; López-Quintela, M.A.; Rivas, J.; Goodenough, J.B. Role of doping and Dimensionality in the Superconductivity of Na_xCoO_2. *Chemistry of Materials*. **2005**, *17*, 1965–1968. https://doi.org/10.1021/cm0500760.
22. Akram, R.; Khan, J.; Rafique, S.; Hussain, M.; Maqsood, A.; Naz, A.A. Enhanced thermoelectric properties of single phase Na doped Na_xCoO_2 thermoelectric material. *Materials Letters*. **2021**, *300*, 130180. https://doi.org/10.1016/j.matlet.2021.130180.
23. Assadi, M.H.N.; Katayama-Yoshida, H. Restoration of long range order of Na ions in Na_xCoO_2 at high temperatures by sodium site doping. *Computational Materials Science*. **2015**, *109*, 308–311. https://doi.org/10.1016/j.commmatsci.2015.07.043.
24. Lee, M.; Viciu, L.; Li, L.; Wang, Y.; Foo, M.L.; Watauchi, S.; Pascal Jr., R.A.; Cava, R.J.; Ong, N.P. Enhancement of thermopower in Na_xCoO_2 in the large-x regime ($x \geq 0.75$). *Physica B*. **2008**, *403*, 1564–1568. https://doi.org/10.1016/j.physb.2007.10.320.
25. Krasutskaya, N.S.; Klyndyuk, A.I.; Evseeva, L.E.; Tanaeva, S.A. Synthesis and properties of Na_xCoO_2 (x = 0.55, 0.89) oxide thermoelectric. *Inorganic Materials*. **2016**, *52*, 393–399. https://doi.org/10.1134/S0020168516030079.
26. Pohle, B.; Gorbunov, M.; Lu, Q.; Bahrami, A.; Nielsch, K.; Mikhailova, D. Structural and electrochemical properties of layered *P*2-$Na_{0.8}Co_{0.8}Ti_{0.2}O_2$ cathode in sodium-ion batteries. *Energies*. **2022**, *15*, 3371. https://doi.org/10.3390/en15093371.
27. Devi Meena, J.; Gayathri, N.; Bharathi, A.; Ramachandran, K. Effect of nickel substitution on thermal properties of $Na_{0.9}CoO_2$. *Bulletin of Materials Science*. **2007**, *30*, 345–348. https://doi.org/10.1007/s12034-007-0057-y.
28. Tian, Z.; Wang, X.; Liu, J.; Lin, Zh.; Hu, Ya.; Wu, Yi.; Han, Ch.; Hu, Zh. Power factor enhancement induced by Bi and Mn co-substitution in Na_xCO_2 thermoelectric materials. *Journal of Alloys and Compounds*. **2016**, *661*, 161–167. https://doi.org/10.1016/j.jallcom.2015.11.084.
29. Ono, Ya.; Kato, N.; Miyazaki, Yu.; Kajitani, T. Transport Properties of Ca-doped γ-Na_xCoO_2. *Journal of Ceramic Society of Japan*. **2004**, *5*, S626–S628. https://doi.org/10.2497/jjspm.50.469.
30. Assadi, M.H.N.; Katayama-Yoshida, H.; Restoration of long order of Na ions in Na_xCoO_2 at high temperatures by sodium site doping. *Computational Materials Science*. **2015**, *109*, 308–311. https://dx.doi.org/10.1016/j.commatsci.2015.07.043.
31. Yang, X.; Wang, X.; Liu, Ju.; Hu, Zh. Power factor enhancement in Na_xCoO_2 doped by Bi. *Journal of Alloys and Compounds*. **2014**, *582*, 59–63. https://doi.org/10.1016/j.jallcom.2013.08.002.
32. Seetawan, T.; Amornkitbamburg, V.; Burinprakhon, Th.; Maensiri, S.; Kurosaki, K.; Muta, H.; Uno, M.; Yamanaka, Sh. Thermoelectric power and electrical resistivity of Ag-doped $Na_{1.5}Co_2O_4$. *Journal of Alloys and Compounds*. **2006**, *407*, 314–317. https://doi.org/10.1016/j.jallcom.2005.06.032.
33. Hussein, M.; Assadi, N. Hf doping for enhancing the thermoelectric performance in layered $Na_{0.75}CoO_2$. *Materials Today: Proceedings*. **2021**, *42*, 1542–1546. https://doi.org/10.1016/j.matpr.2020.01.349.
34. Nakhowong R. Effect of reduced graphene oxide on the enhancement of thermoelectric power factor of γ-$Na_xCo_2O_4$. *Materials Science &Engineering B*. **2020**, *261*, 114679. https://doi.org/10.1016/j.mseb.2020.114679.
35. Ito, M.; Nagira, T.; Furumoto, D.; Katsuyama, Sh.; Nagai, H. Synthesis of Na_xCoO_2 thermoelectric oxides by the polymerized complex method. *Scripta Materialia*. **2003**, *48*, 403–408. https://doi.org/10.1016/j.mseb.2020.114679.
36. Suan, M.S.M.; Farhan,M.A.; Lau, K.T.; Munawar, R.F.; Ismail, S. Structural and Electrical Properties of Na_xCoO_2 Thermoelectric Synthesized via Citric-Nitrate Auto-Combustion Reaction. *Journal of Physics: Conference Series*. **2018**, *1082*, 012033 (6 pages). https://doi.org/10.1088/1742-6596/1082/1/012033.
37. Matsubara, Ic.; Zhou, Yu.; Takeuchi, T.; Funahashi, R.; Shikano, M.; Murayama, N.; Shin, W.; Izu, N. Thermoelectric Properties of Spark-Plasma-Sintered $Na_{1+x}CoO_2$ Ceramics. *Journal of Ceramic Society of Japan*. **2003**, *111*, 238–241. https://doi.org/ 10.1007/s11664-010-1492-x.

 doi:10.20944/preprints202503.0767.v1

38. Park, K.; Jang, K.U.; Know, H.–C.; Kim, J.–G.; Cho, W.–S. , Y. Influence of partial substitution of Cu for Co on the thermoelectric properties of NaCo2O4. *J. of Alloys and Compounds*. **2006**, *419*, 213–219. https://doi.org/10.1016/j.jallcom.2005.08.081.
39. Terasaki, I.; Tsukada, I.; Iguchi, Y. Impurity-induced transition and impurity-enhanced thermopower in the thermoelectric oxide $NaCo_{2-x}Cu_xO_4$. *PHYSICAL REVIEW B*. **2002**, *65*, 195106 (7 pages). https://doi.org/10.1103/PhysRevB.65.195106.
40. Park, K.; Choi, J.W.; Lee, G.W.; Kim, S.–J.; Lim, Y.–S.; Choi, S.–M.; Seo W.–S.; Lim, S.M. Thermoelectric Properties of Solution-Combustion-Processed $Na(Co_{1-x}Ni_x)_2O_4$. *Materials Letters*. **2012**, *18*, 1061–1065. https://doi.org/10.1007/s12540-012-6021-4.
41. Park, K.; Jang, K.U. Improvement in High-Temperature Properties of NaCo2O4 through Partial Substitution of Ni for Co. *Materials Letters*. **2006**, *60*, 1106–1110. https://doi.org/10.1016/j.matlet.2005.10.086.
42. Park, K.; Lee, J.H. Enhanced Thermoelectric Properties of NaCo2O4 by Adding Zn. *Materials Letters*. **2008**, *62*, 2366–2368. https://doi.org/ 10.1016/j.matlet.2007.11.090
43. Klyndyuk A.I., Krasutskaya N.S., Chizhova E.A., Evseeva L.E., Tanaeva S.A. Synthesis and properties of $Na_{0.55}Co_{0.9}M_{0.1}O_2$ (*M* =Sc, Ti, Cr-Zn, Mo, W, Pb, Bi) solid solutions. *Glass Physics and Chemistry*. **2016**, *42*, 100–107, https://doi.org/10.1134/S1087659616010053.
44. Klyndyuk, A.I.; Krasutskaya, N.S.; Dyatlova, E.M. Influence of sintering temperature on the properties of Na_xCoO_2 ceramics. *Proceedings of BSTU.* **2010**, *XVIII*, 99–102 (in Russian).
45. Pyatnitsky, I.V. Analitical chemistry of cobalt. Science: Moscow, **1965**, 292 p (in Russian).
46. Sopicka-Lizer, M.; Kozłowska, K.; Bobrowska-Grzesik, E.; Plewa, J.; Altenburg, H. Assessment of Co(II), Co(III) and Co(IV) content in thermoelectric cobaltites. *Arhives of Metallurgy and Materials*. **2009**, *54*, 881–888.
47. Azad, S.; Kumar, N.; Chand, S. Structural, morphological, optical and dielectric properties of $Ti_{1-x}Fe_xO_2$ nanoparticles sythesized using sol-gel method. *Journal of Sol-Gel Science and Technology*. **2022**, *105*, 1–13, https://doi.org/10.1007/s10971-022-05973-z.
48. Marwah, T.J. Using the size strain plot method to specity lattice parameters. *Haitham Journal for Pure and Applied Science*. **2023**, *36*, 123–129, https://doi.org/10.30526/36.1.2891.
49. Lotgering, F.K. Topotactical reactions with ferrimagnetic oxides having hexagonal crystal structures. *Journal of Inorganic and Nuclear Chemistry*. **1959**, *9*, 113 – 123, https://doi.org/10.1016/0022-1902(59)80070-1.
50. Klyndyuk, A.I.; Chizhova, E.A.; Latypov, R.S.; Shevchenko S.V.; Kononovich, V.M. Effect of the addition of copper particles on the thermoelectric properties of the $Ca_3Co_4O_{9+\delta}$ ceramics produced by two-step sintering. *Inorganic Materials*. **2022**, *67*, 237–244. https://doi.org/10.1134/S0036023622020073.
51. Klyndyuk, A.I.; Petrov, G.S.; Poluyan, A.F.; Bashkirov, L.A. Structure and Physicochemical Properties of $Y_2Ba_{1-x}M_xCuO_5$ (*M* = Sr, Ca) Solid Solutions. *Inorganic Materials*. **1999**, *35*, 512–516. https://doi.org/10.1002/chin.199948024.
52. Zorkovská, A.; Feher, A.; Sébek, J.; Šantavá, E.; Bradaric, I. Non-Fermi-liquid behavior in the layered Na_xCoO_2. *Low Temperature Physics.* **2007**, *33*, 944–947. https://doi.org/10.1063/1.2747070.
53. Snyder, G.J., Ursell, T.S. Thermoelectric Efficiency and Compatibility. *Physical Review Letters*. **2003**, *91*, 148301 (4 pages).
54. Delmas C., Braconnier J.-J., Fouassier C., Hagenmuller P. Electrochemical intertcalation of sodium in Na_xCoO_2 bronzes. *Solid State Ionics*. **1981**, *3*, 165–169. https://doi.org/ 10.1016/0167-2738(81)90076-X.
55. Liu, P.; Chen, G.; Cui, Y.; Zhang, H.; Xiao, F.; Wang, L.; Nakano, H. High temperature electrical conductivity and thermoelectric power of Na_xCoO_2. *Solid State Ionics*. **2008**, *179*, 2308–2312. https://doi.org/10.1016/j.ssi.2008.08.010
56. Matsubara, I.; Zhou, Yu.; Takeuchi, T.; Funahashi, R.; Shikano, M.; Murayama, N.; Shin, W.; Izu, N. Thermoelectric properties of spark-plasma-sintered $Na_{1+x}Co_2O_4$ ceramics. *Journal of Ceramic Society of Japan*. **2003**, *111*, 238–241.
57. Li, N.; Jiang, Ya.; Li, G.; Wang, Ch.; Shi, J.; Yu D. Self-ignition route to Ag-doped $Na_{1.7}Co_2O_4$ and its thermoelectric properties. *Journal of Alloys and Compounds*. **2009**, *467*, 444–449. https://doi.org/10.1016/j.jallcom.2007.12.012.

 doi:10.20944/preprints202503.0767.v1

58. Yang, X.; Wang, X.; Liu, J.; Hu Zh. Power factor enhancement in Na_xCoO_2 doped by Bi. *Journal of Alloys and Compounds*. **2014**, *582*, 59–63. https://doi.org/10.1016/j.jallcom.2013.08.002.
59. Baster, D.; Zając, W.; Kondracki, Ł.; Hartman, F.; Molenda, J. Improvement of electrochemical performance of $Na_{0.7}Co_{1-y}Mn_yO_2$–cathode material for rechargeable sodium-ion batteries. *Solid State Ionics*. **2016**, *288*, 213–218. https://doi.org/10.1016/j.ssi.2016.01.003.
60. Klyndyuk A.I., Matsukevich I.V. Synthesis, structure and properties of $Ca_3Co_{3.85}M_{0.15}O_{9+\delta}$ (M – Ti–Zn, Mo, W, Pb, Bi). *Russian Journal of Inorganic Chemistry*. **2015**, *51*, 1025–1031. https://doi.org/10.1134/S0020168515080105.
61. Lin, Y.-H.; Lan, J.; Shen, Z.; Liu, Y.; Nan, C.-W.; Li, J.-F. High-temperature electrical transport behaviors in textured $Ca_3Co_4O_9$-based polycrystalline ceramics, *Appl. Phys. Lett*. **2009**, *94*, 072107. https://doi.org/10.1063/1.3086875
62. Zhang, W.; Zhu, K.; Liu, J.; Wang, J.; Yan, K.; Liu, P.; Wang, Y. Influence of the phase transformation in Na_xCoO_2 ceramics on thermoelectric properties. *Ceramics International*. **2018**, *44*, 17251–17257. https://doi.org/10.1016/j.ceramint.2018.06.183.
63. Snyder, G.J.; Snyder, Al. H.; Wood, M; Gurunathan, R.; Snyder, B.H.; Niu Ch. Weighted Mobility. *Advanced Materials*. **2020**. 2001537 (5 pages). https://doi.org/10.1002/adma.202001537.
64. Wang, Sh.; Chen, Sh.; Liu, F.; Yan, G.; Chen, J.; Li, H.; Wang, J.; Yu, W.; Fu, G. Laser-induced voltage effects in *c*-axis inclined Na_xCoO_2 thin films. *Applied Surface Science*. **2012,** *258*, 7330–7333. https://10.1016/j.apsusc.2012.03.186
65. Liu, W., Tang, X., Sharp, J. Low-temperature solid state synthesis and thermoelectric properties of high-performance and low-cost Sb-doped $Mg_2Si_{0.6}Sn_{0.4}$. *Journal of Physics D: Applied Physics*. **2010**, *43*, 085406 (6 pages). https://doi.org/10.1088/0022-3727/43/8/085406.